

# Overview of dust explosibility characteristics

Kenneth L. Cashdollar \*

*Pittsburgh Research Laboratory, National Institute for Occupational Safety and Health, Pittsburgh, PA, USA*

---

## Abstract

This paper is an overview of and introduction to the subject of dust explosions. The purpose is to provide information on the explosibility and ignitability properties of dust clouds that can be used to improve safety in industries that generate, process, use, or transport combustible dusts. The requirements for a dust explosion are: a combustible dust, dispersed in air, a concentration above the flammable limit, the presence of a sufficiently energetic ignition source, and some confinement. An explosion of a fuel in air involves the rapid oxidation of combustible material, leading to a rapid increase in temperature and pressure. The violence of an explosion is related to the rate of energy release due to chemical reactions relative to the degree of confinement and heat losses. The combustion properties of a dust depend on its chemical and physical characteristics, especially its particle size distribution. In this paper, the explosion characteristics of combustible dusts will be compared and contrasted with those of flammable gases, using methane as an example. These characteristics include minimum explosible concentration, maximum explosion pressure, maximum rate of pressure rise, limiting oxygen concentration, ignition temperature, and amount of inert dust necessary to prevent flame propagation. The parameters considered include the effects of dust volatility, dust particle size, turbulence, initial pressure, initial temperature, and oxygen concentration. Both carbonaceous and metal dusts will be used as examples. The goal of this research is to better understand the fundamental aspects of dust explosions. Published by Elsevier Science Ltd.

*Keywords:* Dust; Explosibility; Explosion

---

## 1. Introduction

In industries that manufacture, process, generate, or use combustible dusts, an accurate knowledge of their explosion hazards is essential. Various books have been published since 1980 on the general subject of the explosion hazards of dusts and powders (Bartknecht 1981, 1989, 1993; Field, 1982; Nagy & Verakis, 1983; Cashdollar & Hertzberg, 1987; Eckhoff, 1991). The present paper is an update of a previous Pittsburgh Research Laboratory<sup>1</sup> (PRL) paper (Hertzberg & Cashdollar, 1987) on the general topic of the explosion hazards of dusts. The basic variables that influence the characteristics of a dust explosion will be discussed in general terms without specific reference to particular practical systems. One purpose of this paper is to provide assistance and guidance to the practising safety engineer at a plant regarding the important variables in dust

explosibility. Both carbonaceous and metal dusts are used as examples of combustible dusts. Although many of the examples in this paper use coal dust, the concepts are applicable to other dusts as well.

This paper is not meant to be an overview of the many areas of dust explosion research throughout the world. Instead, it is only meant to be an overview of some of the dust explosibility characteristics that are important for safety engineers to consider at industrial plants.

## 2. Dust explosion requirements

The three requirements for combustion are a fuel, an oxidizer (usually air), and an adequate heat or ignition source. This is often called the “fire triangle”. The fuel can be any material capable of reacting rapidly and exothermically with an oxidizing medium. In this case, the fuel is a combustible dust. For a dust explosion, the dust must be dispersed in the air at the same time that the ignition source is present. The resulting rapid oxidation of the fuel dust leads to a rapid increase in temperature and therefore pressure. This explosion may be a deflagration or a detonation, depending on the rate of reaction

---

\* Tel.: +1-412-386-6753; fax: +1-412-386-6595.

*E-mail address:* kgc0@cdc.gov (K.L. Cashdollar).

<sup>1</sup> The Pittsburgh Research Laboratory was part of the U.S. Bureau of Mines before transferring to the National Institute for Occupational Safety and Health (NIOSH) in October 1996.

and resulting burning velocity. The discussion in this paper is mainly confined to deflagrations. The destructive pressure forces of an explosion can destroy structures and endanger personnel. The violence of an explosion is dependent on the rate of energy release due to chemical reactions relative to the degree of confinement and heat losses. The requirements for a dust explosion are often called (Stephan, 1990) the “explosion pentagon”—consisting of fuel, dispersion/suspension, oxidizer, heat/ignition source, and confinement. The confinement is usually the walls of the equipment or building in which the dust is dispersed, but it could also come from self-confinement if the reaction is fast enough. It is possible to have a destructive explosion even in open air if the reaction is so fast that pressure builds up in the dust cloud faster than it can be released at the edge of the cloud.

Whether the reacting material is a gas or a dust, the combustion products are usually gases so that the explosion process in a closed system is most simply understood in terms of the ideal gas law:

$$PV = nRT = \frac{m}{M}RT \quad (1)$$

where the absolute pressure,  $P$ , times the system volume,  $V$ , is proportional to the temperature,  $T$ . The proportionality constants are the number of moles,  $n$ , and the universal gas constant,  $R$ . The number of moles is equal to the mass of gas,  $m$ , divided by the average molecular weight,  $M$ . For a typical accidental explosion, air is usually the oxidant and the fuel may be a dust, gas, or hybrid mixture. Because air consists mainly of nitrogen, there is usually little change in the number of moles of gas during combustion. Therefore, to a first approximation, a rapid combustion reaction in a closed system results in:

$$\frac{P_{\max}}{P_0} = \frac{T_b}{T_0} \quad (2)$$

where  $P_{\max}$  is the maximum absolute explosion pressure,  $P_0$  is the initial absolute pressure,  $T_b$  is the absolute temperature of the burned gas and  $T_0$  is the initial absolute temperature. The faster the combustion reaction is, the more adiabatic the system will be, and the more nearly will the explosion pressure approximate the ideal relation in Eq. (2). If the number of moles of gas changes significantly during combustion or if the explosion vents from the container volume, the maximum explosion pressure will be significantly changed.

In this paper, the terms “flammability” and “explosibility” are used interchangeably to refer to the ability of an airborne dust cloud and/or gas mixture to propagate a deflagration after it has been initiated by a sufficiently strong ignition source. Historically, the term “flammability” has been used more often for gases, and “explosibility” more often for dusts.

The mechanism of flame propagation for many dusts is combustion of flammable gases emitted by particles heated to the point of vaporization or pyrolysis (Hertzberg, Zlochower & Cashdollar, 1988b; Cashdollar, Hertzberg & Zlochower, 1989). Some other dusts can propagate a flame through direct oxidation at the particle surface (Hertzberg, Zlochower & Cashdollar, 1992). For either mechanism, a finer size of dust is likely to react faster than a larger size of dust of the same material. Particle shape and porosity can also greatly affect the particle surface area and the reaction rates. Therefore, the dust particle size and shape are of primary importance in regard to dust explosibility characteristics. Dusts are often defined as material that is minus 20 mesh (<850  $\mu\text{m}$ ) (Stephan, 1990; Nagy, 1981) or minus 40 mesh (<420  $\mu\text{m}$ ) (NFPA, 1998). However, the larger dust particles participate inefficiently in the flame propagation process. It is the finer fraction of the dust particles that contributes the most to the hazard because the finer particles have a greater surface area per mass and therefore react faster. The finer dust particles are also more easily dispersed in air and remain airborne longer.

An example of a dust particle size distribution is shown in Fig. 1. The cumulative distribution is shown in Fig. 1A and the differential distribution in Fig. 1B as semi-logarithmic plots. The two types of size distributions are shown both as surface area weighted and as mass or volume weighted curves. The surface median

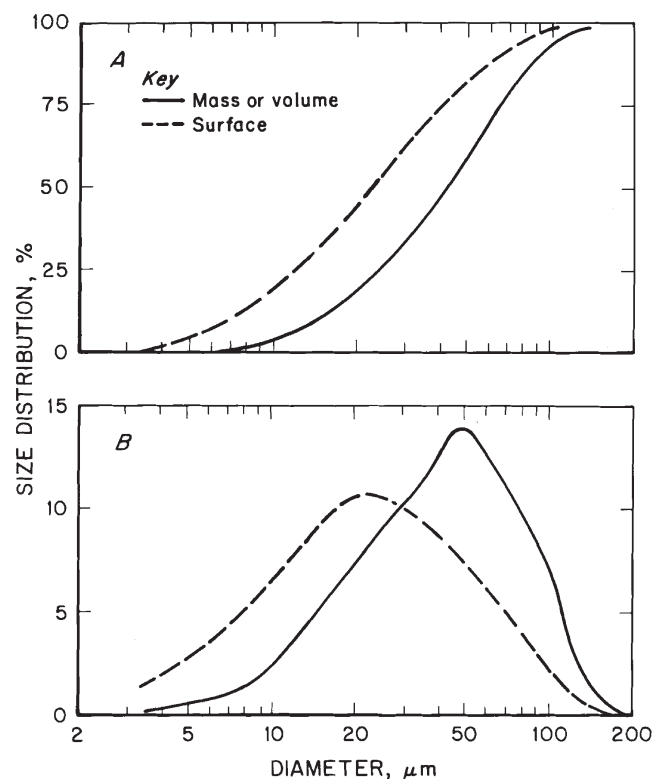


Fig. 1. Dust particle size distributions by surface area and mass: (A) cumulative distribution; (B) differential distribution.

diameter (23  $\mu\text{m}$ ) and the mass median diameter (42  $\mu\text{m}$ ) can be determined from the 50% points on the cumulative curves in Fig. 1A. The cumulative curve also shows that the dust has 82% by mass minus 200 mesh (<75  $\mu\text{m}$ ). The differential curves in Fig. 1B are often more useful in visualizing the size distribution. Other ways of identifying a representative particle size for the dust in Fig. 1 are the surface mean diameter ( $\bar{D}_s=30 \mu\text{m}$ ) and the mass mean diameter ( $\bar{D}_w=50 \mu\text{m}$ ), calculated from the data in Fig. 1B. Because the combustion of the dust cloud is greatly dependent on the surface area of the dust, a mean particle diameter based on surface area is perhaps more appropriate than one based on mass. Various books on particle size analysis (e.g. Allen, 1975; Irani & Callis, 1963), may be useful in better understanding this aspect of dusts. It should be noted that different particle size analysis instrumentation may give somewhat different results for the same dust because of the different particle sizing methods used.

The combustion properties of a dust depend on its chemical and physical characteristics, especially its particle size distribution. Published dust explosibility data can give an indication of the hazards associated with a particular type of dust. However, it is preferable to determine the explosibility characteristics of an industrial dust by test, because published data are for a particular size distribution that may be different from the dust in question. Particle shape and porosity are also important considerations in the explosibility of a dust. In general, shapes with greater surface area will propagate flame more readily and therefore be more hazardous.

It should be noted that there is no US standardized test for whether or not a dust is explosible. There are tests to determine whether a dust can be ignited by an electric spark (Dorsett, Jacobson, Nagy & Williams, 1960) or what the maximum explosion pressures (ASTM, 1999a) or minimum explosible concentrations (ASTM, 1999b) are using stronger chemical ignitors. One reason for this lack of an explosibility test is that the question of whether or not a dust can be ignited and propagate a flame depends greatly on the ignition source. However, different industries have different views about what would be an appropriate or likely ignition source. For some industries, it could be an electrostatic spark; for others, it could be a flame; and for the mining industry, it could be a very large flame from blown-out explosives. Therefore, each industry has to decide what are the likely or possible ignition sources and which dusts could be ignited by them.

### 3. Laboratory equipment for dust explosibility evaluation

The explosibility characteristics of dust clouds are often measured in closed volume chambers. The 1.2-L

Hartmann tube (Nagy & Verakis, 1983; Dorsett et al., 1960) is often used for preliminary screening tests and for minimum ignition energy (MIE) measurements. However, it may yield false negatives for dusts that are difficult to ignite with a spark but that are ignitable by stronger ignition sources. It is also not recommended (ASTM, 1999a) for measuring rates of pressure rise. The 20-L chambers are used for explosibility measurements such as maximum explosion pressures, maximum rates of pressure rise, minimum explosible concentrations, and inerting effects. An example of a 20-L laboratory chamber (Cashdollar & Hertzberg, 1985) is shown in Fig. 2. This is the standard laboratory test chamber designed and used at the PRL for studying the explosibility and inerting of combustible dusts. There is another style of 20-L chamber designed by R. Siwek (Bartknecht 1981, 1989; Siwek 1977, 1985, 1988) that is in wide use in Europe and elsewhere. There are also 1-m<sup>3</sup> (1000-L) chambers (Bartknecht 1981, 1989; Cashdollar & Chatrathi, 1993). The 1-m<sup>3</sup> chambers may give more realistic measurements of minimum explosible concentrations, maximum explosion pressures, and maximum rates of pressure rise, but the testing is more time consuming and requires much larger dust samples than the 20-L chambers.

The PRL 20-L chamber is made of stainless steel, and has a pressure rating of 21 bar. Two optical dust probes (Cashdollar, Liebman & Conti, 1981; Conti, Cashdollar & Liebman, 1982) are used to measure the uniformity of the dust dispersion at the positions shown in Fig. 2. The optical probes measure the transmission through the dust cloud, with path lengths of 38 or 95 mm. The strain gauge pressure transducer measures the explosion pressure and rate of pressure rise (dP/dt). The data from the various instruments are collected by a high speed personal computer (PC) based data acquisition system. The experimental dust concentration reported for the 20-L chamber is the mass of dust divided by the chamber volume. After the dust and ignitor have been placed in the chamber, the chamber is partially evacuated to an absolute pressure of 0.14 bar,a. Then a short blast of dry air (from a reservoir at ~9 bar) disperses the dust and raises the chamber pressure to about 1 bar,a. There is a total ignition delay of ~0.4 s from the start of dispersion until ignition for the standard test procedure in the PRL 20-L chamber. The standard procedure for the Siwek 20-L chamber has an ignition delay of ~0.06 s and a reservoir pressure of 20 bar, resulting in a higher level of turbulence. The usual ignition sources used for the 20-L tests are electrically activated, pyrotechnic ignitors manufactured by Fr. Sobbe<sup>2</sup> of Germany. These ignitors are available in various energies from 250 to 10,000 J.

<sup>2</sup> Mention of any company name or product does not constitute endorsement by NIOSH.

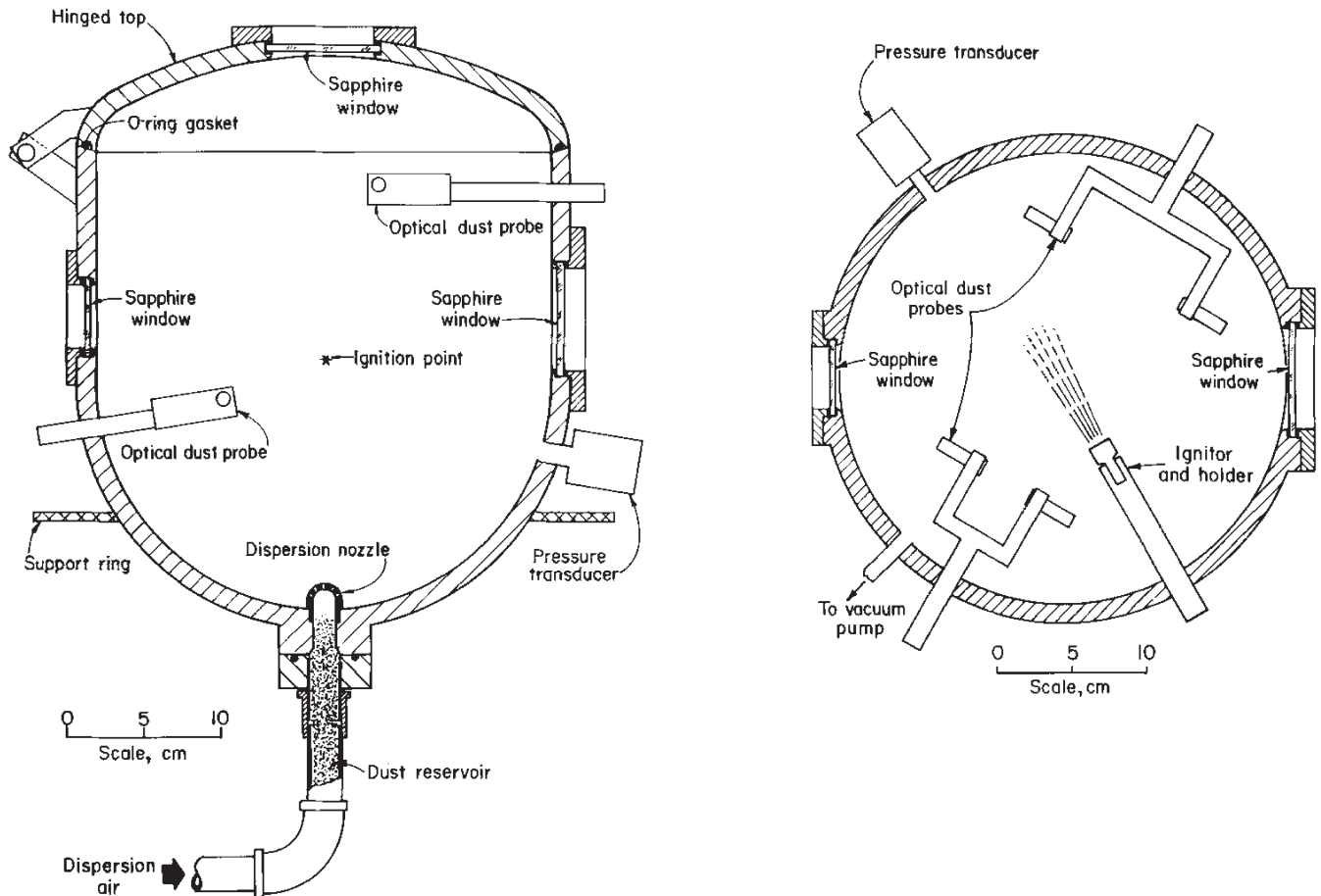


Fig. 2. Vertical and horizontal cross sections of PRL 20-L explosibility test chamber.

The 2500-J ignitor is comparable in energy to an entire book of 20 pocket matches, all ignited at once. The Sobbe ignitors are much stronger than the electric sparks used in the 1.2-L Hartmann tests.

#### 4. Explosion characteristics

##### 4.1. Pressures and rates of pressure rise

Examples of the pressure data for a weak and a moderate coal dust explosion are shown in Figs. 3 and 4.

The absolute pressure (Figs. 3A and 4A) and rate of pressure rise (Figs. 3B and 4B) are plotted versus time. Fig. 3 shows the data for a 20-L chamber explosion test of a low volatile bituminous coal at a dust concentration of  $125 \text{ g/m}^3$ , which is just above the minimum required for an explosion. The pressure trace in Fig. 3A starts at the partially evacuated value of 0.14 bar,a. The blast of air that disperses the dust starts at 0.1 s and ends at 0.4 s on the pressure–time trace. The ignitor is activated at 0.5 s at a chamber pressure of 1.0 bar,a. The maximum explosion pressure is about 3 bar,a or a pressure rise of about 2 bar. In Fig. 3B, the rate of pressure rise,

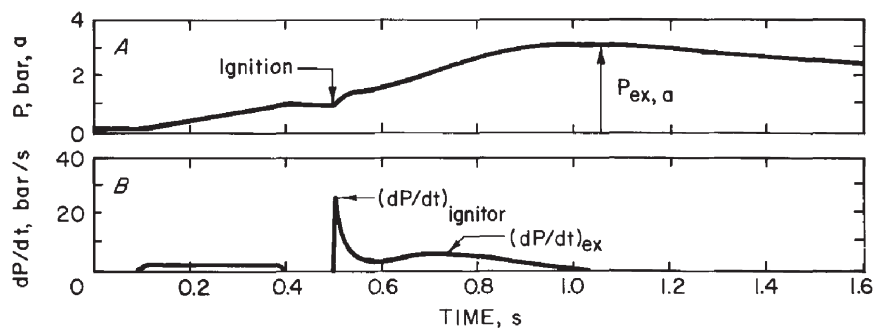


Fig. 3. Typical pressure data for a weak dust explosion.

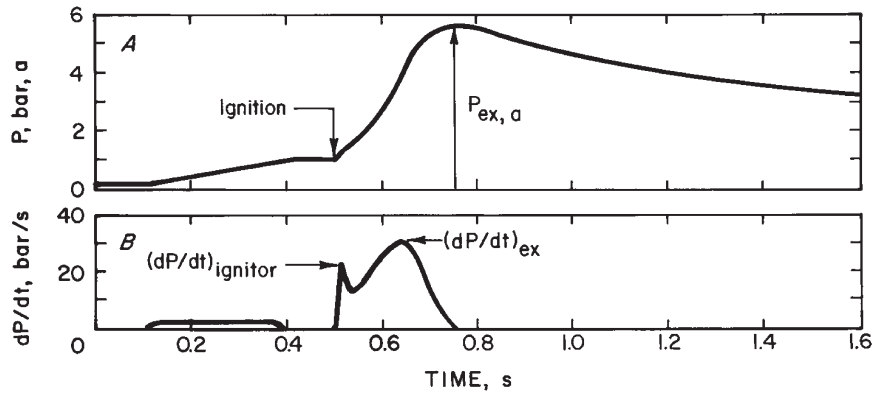


Fig. 4. Typical pressure data for a moderate dust explosion.

$(dP/dt)_{\text{ignitor}}$ , for the ignitor is larger than  $(dP/dt)_{\text{ex}}$  for the dust explosion itself. It is important to determine  $(dP/dt)_{\text{ex}}$  rather than the ignitor effects. Fig. 4 shows data for a larger explosion of the low volatile coal dust at a higher concentration of  $200 \text{ g/m}^3$ . The maximum explosion pressure is about 5.5 bar, a or a pressure rise of 4.5 bar. For this explosion, the  $(dP/dt)_{\text{ex}}$  for the dust explosion is greater than  $(dP/dt)_{\text{ignitor}}$ .

Examples of absolute pressure versus time traces for typical dust explosions at a concentration of  $600 \text{ g/m}^3$  in the constant volume 20-L chamber are shown in Fig. 5. The traces are for two carbonaceous dusts and six metal dusts. The relative reactivity of the dusts can be estimated from either the peak explosion pressure or the maximum rate of pressure rise. The aluminum (Al) has the highest reactivity, in part because it is much finer in size than any of the other dusts in Fig. 5. Next in order

of reactivity is the magnesium (Mg) dust, followed by the two carbonaceous dusts (polyethylene and coal). The polyethylene and the high volatile bituminous coal (hvb) have similar maximum pressures, but the polyethylene has a faster rate of pressure rise. The titanium (Ti) dust has a lower explosion pressure than the carbonaceous dusts, and the iron (Fe) and zinc (Zn) dusts are even lower. The dust with the lowest reactivity in Fig. 5 is the tantalum (Ta) dust, which barely reaches its maximum pressure by 250 ms. The relative reactivities of these dusts are dependent not only on the intrinsic reactivities of the materials but also on the specific particle sizes of the dusts.

The pressure evolution of an explosion in a constant volume system is predicted by classical combustion theory (Lewis & von Elbe, 1961, pp. 367–381). For the ideal case, the absolute pressure as a function of time,

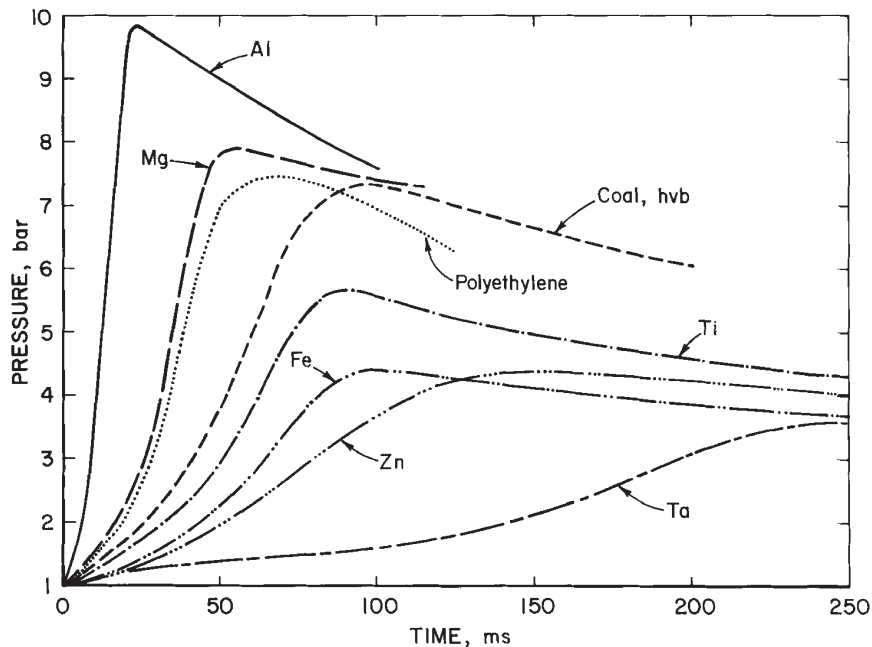


Fig. 5. Explosion pressure traces for carbonaceous and metal dusts.

$P(t)$ , in a constant volume, spherical explosion is related to the fractional volume,  $V(t)$ , occupied by the fireball during the time of propagation,  $t$ , as follows (Hertzberg & Cashdollar, 1987):

$$\frac{P(t)-P_0}{P_{\max}-P_0} = k \frac{V(t)}{V_0} \quad (3)$$

where  $P_0$  is the initial absolute pressure,  $V_0$  is the chamber volume, and  $k$  is a correction factor related to the difference in compressibility between burned and unburned gases. For spherical propagation from a point source,

$$\frac{V(t)}{V_0} = \left[ \frac{r(t)}{r_0} \right]^3 = \left[ \frac{S_b t}{r_0} \right]^3 \quad (4)$$

where  $r(t)$  is the fireball radius,  $r_0$  is the chamber radius, and  $S_b$  is the flame speed given by:

$$S_b = \frac{dr(t)}{dt} = \left( \frac{\rho_u}{\rho_b} \right) S_u \quad (5)$$

where  $\rho_u/\rho_b$  is the density ratio of unburned to burned gases (at constant pressure). The burning velocity,  $S_u$ , is the rate of flame propagation relative to the unburned gas ahead of it. The flame speed,  $S_b$ , is relative to a fixed reference point. Note that both  $S_b$  and  $S_u$  are for turbulent not laminar conditions for dust explosions. For spherical propagation in a spherical chamber, the maximum pressure is reached just as the flame contacts the wall. At that instant,  $k=1$ . Differentiating Eq. (3) with respect to time and substituting Eqs. (4) and (5) into the results gives:

$$\begin{aligned} \frac{dP(t)}{dt} &= 3(P_{\max}-P_0) \frac{r(t)^2 dr(t)}{r_0^3 dt} \\ &= 3(P_{\max}-P_0) \left( \frac{\rho_u}{\rho_b} \right) S_u \frac{r(t)^2}{r_0^3} \end{aligned} \quad (6)$$

Eq. (6) shows that the maximum rate of pressure rise should also occur at the instant the flame front contacts the wall. Setting  $r(t)=r_0=(3V_0/4\pi)^{1/3}$  and letting  $\rho_u/\rho_b \approx T_b/T_0 \approx P_{\max}/P_0$ , gives:

$$K_{St} = \left[ \frac{dP(t)}{dt} \right]_{\max} V_0^{1/3} = 4.84 \left( \frac{P_{\max}}{P_0} - 1 \right) P_{\max} S_u \quad (7)$$

Eq. (7) is the ‘‘cubic law’’, and  $K_{St}$  is the size normalized maximum rate of pressure rise.<sup>3</sup> The subscript ‘‘St’’ refers to Staub, the German word for dust. Because it is size normalized, the  $K_{St}$  value is used in the practical design of venting systems (NFPA, 1998).

This derivation of the ‘‘cubic law’’ is based on the idealized condition where the vessel size is large compared with either the dust flame thickness or the ignitor flame

volume. This may be approximately true in the 1-m<sup>3</sup> chambers. However, in the 20-L chambers with pyrotechnic ignitors, it is certainly not true, and the ignition and combustion are more volumetric (Zhen & Leuckel, 1997).

#### 4.2. Dust concentration effects

In order to study the overall explosibility characteristics of a dust, tests must be made over a range of concentrations to determine the ‘‘worst case’’. Explosibility data for the high volatile Pittsburgh bituminous coal dust are shown in Fig. 6 as a function of dust concentration. At the top of the figure, the transmission data measured by the optical dust probes are shown. The transmission is measured over a 0.1-s time interval just before the dust is ignited. As described in Cashdollar et al. (1981) and Conti et al. (1982), the transmission  $\tau$  is related to the mass concentration  $C_m$  by Bouguer’s law:  $\tau = \exp(-3QC_m \ell / 2\rho \bar{D}_s)$ , where  $Q$  is a dimensionless

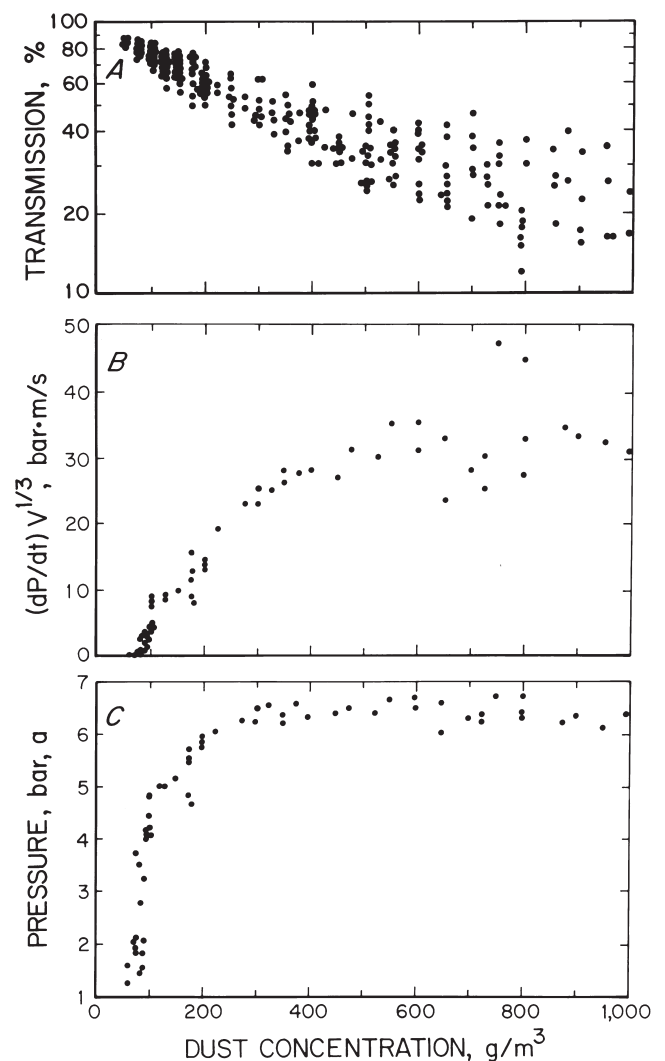


Fig. 6. Explosibility data for high volatile bituminous coal dust.

<sup>3</sup> Note that this equation has been corrected from the version in eq. (7) in Hertzberg & Cashdollar (1987).

extinction coefficient,  $\ell$  is the path length,  $\rho$  is the density of a particle, and  $\bar{D}_s$  is the surface mean particle diameter. The data in Fig. 6A generally follow the expected linear relationship on this semi-logarithmic plot. At the highest dust concentrations, there is some upward curvature, probably due to increased agglomeration. The scatter in the data is probably due to variations in the agglomerated particle size of the air dispersed dust.

In Fig. 6B,  $(dP/dt)V^{1/3}$  is the volume normalized maximum rate of pressure rise. Note that the turbulence level was lower in the PRL 20-L chamber for these tests than that recommended in ASTM E1226 (ASTM, 1999a). Therefore, the  $(dP/dt)V^{1/3}$  data in Fig. 6B are not recommended for the sizing of vents according to ISO Standard 6184/1 (ISO, 1985), NFPA Guide 68 (NFPA, 1998), and VDI Standard 3673 (VDI, 1983). These consensus standards are based on the higher turbulence level of the Siwek 20-L chamber and the 1-m<sup>3</sup> chamber (Bartknecht 1981, 1989). These PRL 20-L data are, however, useful as a relative measure of explosion hazard. At the higher turbulence level recommended in ASTM Standard E1226, the maximum  $(dP/dt)V^{1/3}$  data for this Pittsburgh coal would be roughly three times higher. The maximum absolute explosion pressures (with the pressure rise of the ignitor subtracted) are shown in Fig. 6C. Because there are small variations from test to test in the chamber pressure at the time of ignition, these data were normalized to a starting pressure of 1.0 bar. The data in Fig. 6 show that below a certain dust concentration, explosions are not observed. This is the minimum explosible concentration (MEC) or lean flammable limit (LFL). For this coal, the measured MEC in the 20-L chamber is  $\sim 80$  g/m<sup>3</sup>. This is the same as the  $\sim 80$  g/m<sup>3</sup> MEC-value measured for the same coal in a 1-m<sup>3</sup> chamber using a 10-kJ ignitor (Cashdollar & Chatrathi, 1993; Cashdollar, Weiss, Greninger & Chatrathi, 1992). At higher dust concentrations in Fig. 6, the maximum pressures and rates of pressure rise level off as all of the oxygen in the chamber is consumed, but there is no evidence of a rich limit for the coal dust. Typical of dusts, there is more scatter in the rate of pressure rise data than in the pressure data.

A summary of the 20-L chamber pressure versus concentration data for the bituminous coal and polyethylene dusts is shown in Fig. 7, where the data are compared with those for methane (CH<sub>4</sub>) gas. The data for the two carbonaceous dusts are similar, except that the polyethylene has a lower MEC and a slightly higher maximum explosion pressure. This is because the polyethylene has a volatility of 100% compared with 37% volatility for the coal, and it has a higher H:C ratio than the coal. The methane gas has a LFL or MEC similar to that of the polyethylene. This shows that the completely volatilizable polyethylene reacts similarly to the methane gas at low concentrations (Hertzberg et al., 1988b). For

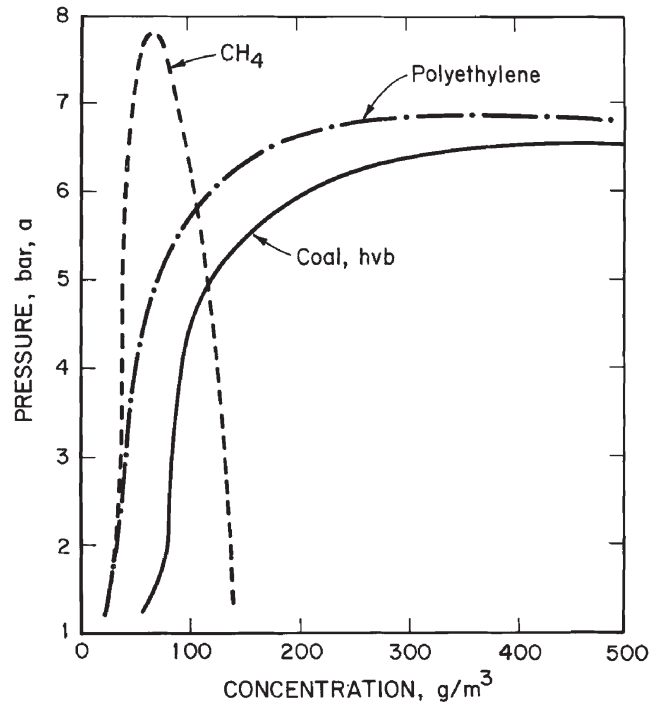


Fig. 7. Explosion pressure data for high volatile bituminous (hvb) coal and polyethylene dusts, compared with those of methane gas.

hydrocarbon gases or dusts, the measured LFL or MEC generally corresponds to a calculated adiabatic temperature (Hertzberg et al., 1988b) of 1300 to 1500 K. This is the “limit flame temperature”, which is the minimum temperature needed to keep a flame propagating. Experimentally, the LFLs of most hydrocarbon gases are easy to measure because the gases have low ignition energies. Much stronger ignition energies are needed for dusts (Cashdollar & Chatrathi, 1993; Hertzberg, Cashdollar & Zlochower, 1988a). However, if too strong an ignition energy is used relative to the test chamber volume, the result will be an overdriven ignition (Cashdollar & Chatrathi, 1993). A standard method for measuring the MEC of a dust cloud is ASTM E1515 (ASTM, 1999b).

In contrast to the two dusts in Fig. 7, the methane gas shows a rich limit. For the dusts, the maximum pressures level off at concentrations of 200 to 300 g/m<sup>3</sup> as all of the oxygen in the chamber is consumed. At even higher dust concentrations, although the mixtures are nominally fuel rich, the pressure nevertheless remains constant. The normal rich limit observed for hydrocarbon gases such as CH<sub>4</sub> is not observed for the dusts. An explanation of this effect, at least for many dusts, is that the solid phase fuel must first devolatilize before it can mix with the air (Hertzberg et al., 1988b). As soon as sufficient volatiles are generated to form a stoichiometric concentration of volatiles in air, the flame front propagates rapidly through the mixture before excess fuel volatiles can be generated.

Fig. 8 shows explosibility data from the 20-L chamber

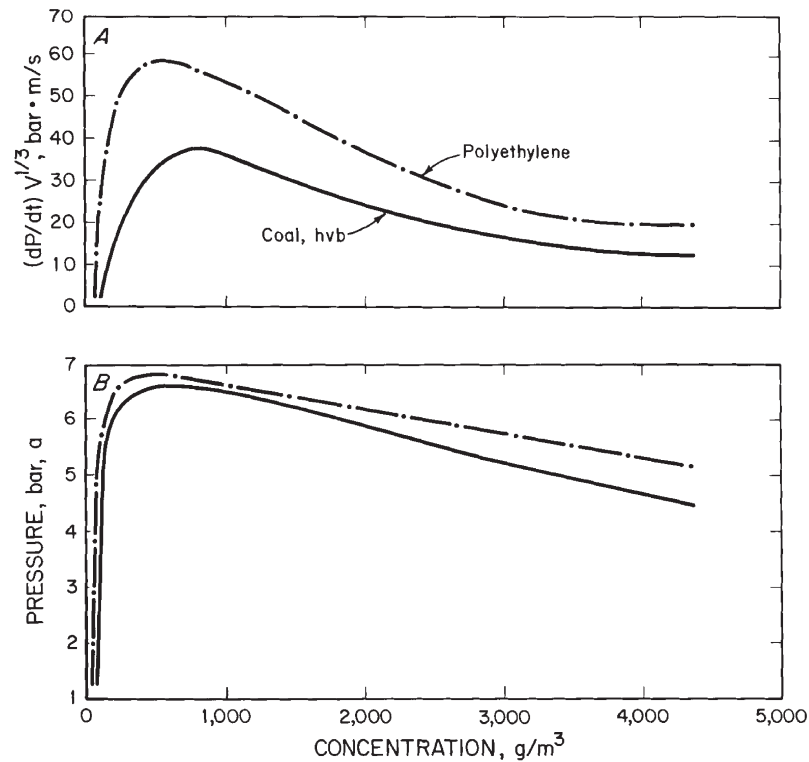


Fig. 8. Explosibility data at very high dust concentrations for high volatile bituminous coal and polyethylene dusts.

with 2500-J ignitors for the high volatile coal dust and for polyethylene dust at very high concentrations. This shows that these dusts explode even at concentrations beyond 4000 g/m<sup>3</sup>. There is, of course, an increased uncertainty in the dust dispersion effectiveness at these very high concentrations. The decrease in pressure at higher concentrations may be due to the increased heat sink of the very large dust concentrations. The decrease in  $dP/dt$  at higher concentrations may be due to the increased heat sink effect and/or to the possible decrease in turbulence due to the large mass of dust. Deguigand & Galant (1981) had previously observed an apparent upper limit at  $\sim 4$  kg/m<sup>3</sup> for coal dust, but this may have been only an ignitability limit because they used an electric spark ignition source that was much weaker than the 2500-J Sobbe ignitor used here. Mintz (1993) observed some upper limits under conditions of reduced oxygen and at large coal particle sizes. In principle, there are rich limits for dusts. Eventually, the large mass of excess fuel will become too much of a heat sink and the flame temperature will be reduced below its limit value. However, for most practical purposes, dusts can be considered to have no rich limit of explosibility. This observation has also been made by Wolanski (1992).

Examples of scanning electron microscope (SEM) photomicrographs of coal before and after explosions are shown in Fig. 9. The dust was a narrow size distribution of Pittsburgh coal with a mass median diameter,  $D_{med} \approx 23$   $\mu\text{m}$ . The original unburned particles are shown

at two magnifications on the left side of the figure. They are compared to the “burned” post-explosion particles in the four frames on the right side of the figure. The burned particles are mainly char residues that are often larger than the original particles. In the flame, the bituminous coal particles become molten as shown by the rounded particles on the right. Some particles form cenospheres. The particles also devolatilize in the flame, and the volatiles are emitted through the “blow holes” seen in the char residues. Additional SEM photomicrographs for various post-explosion dust residues are in Ng, Cashdollar, Hertzberg & Lazzara (1983).

Metal dusts show similar explosibility data to carbonaceous dusts, as shown by the data for two sizes of iron dust in Fig. 10. The Fe-1 dust was finer in size and had  $D_{med} \approx 4$   $\mu\text{m}$ ; the Fe-2 dust had  $D_{med} \approx 45$   $\mu\text{m}$ . The explosion pressures, rates of pressure rise, and measured explosion temperatures are shown as a function of dust concentration. Fig. 10C shows the measured explosion pressure (absolute) for each test, corrected for the pressure rise due to the ignitor. Fig. 10B shows the size normalized maximum rate of pressure rise,  $(dP/dt)V^{1/3}$ , for each explosion test. As for the coal dust data in Fig. 6, the iron data in Fig. 10 show that explosions are not observed below a certain dust concentration. The MECs for the Fe-1 and Fe-2 dusts are about 220 and 500 g/m<sup>3</sup>, respectively, based on the procedures of ASTM E1515 (ASTM, 1999b). However, there is considerable uncertainty in these values, especially for the Fe-2 dust, due

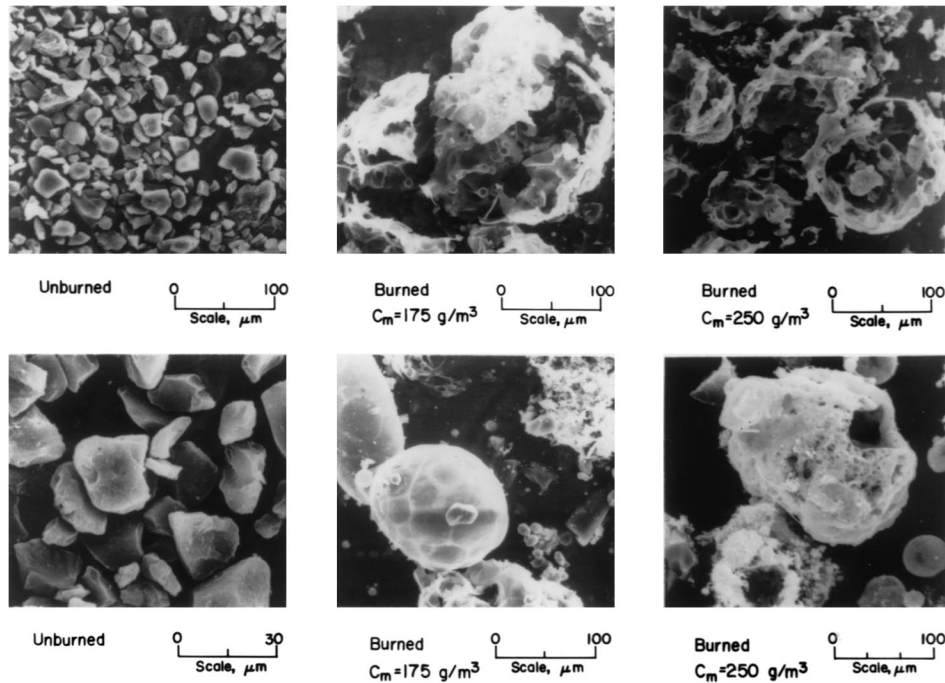


Fig. 9. Scanning electron microscope photographs of bituminous coal particles before and after explosions.

to the scatter in the data. At the higher dust concentrations,  $P_{\max}$  and  $(dP/dt)_{\max} V^{1/3}$  level off as all of the oxygen in the chamber is consumed. Similar to the carbonaceous dusts in Fig. 8, the iron metal dusts show no evidence of a “normal” rich limit.

The explosion temperatures shown in Fig. 10A were measured with a six-wavelength infrared pyrometer (Cashdollar & Hertzberg, 1982). The pyrometer observed the continuum radiation from the particles, and temperatures were calculated from the best Planck curve fit to the infrared radiance data. The maximum measured particle temperatures for the Fe-1 dust were  $\sim 1800 \text{ K}$ , well below the maximum calculated adiabatic temperature,  $T_{\text{ad,max}} = 2250 \text{ K}$ , for ideal combustion at constant pressure (Cashdollar, 1994). The maximum measured particle temperatures for the Fe-2 dust were even lower. These experimental temperatures are only those of the particles in the explosion; the gas temperatures may be different. For all three explosion characteristics shown in Fig. 10, the Fe-1 dust has higher values than the Fe-2 dust, showing that it is more reactive, due to its finer particle size.

#### 4.3. Particle size effects

Most of the previous explosibility data were measured using rather broad size distributions of the dusts. Fig. 11 shows explosibility data from the 20-L chamber for Pittsburgh bituminous coal dust as a function of mass median particle diameter. The data for the narrow size distributions are shown as the solid circles and solid curve. These data for narrow distributions are compared

with the data crosses for the broad size distributions of coal dusts. The MEC-values in the bottom section of the figure are relatively independent of particle size for the finer sizes. At the larger sizes, above  $100 \mu\text{m}$ , the MEC-values increase with particle size until a size is reached that can not be ignited. The top two sections of Fig. 11 show that the maximum pressures and rates of pressure rise are found at the finest sizes tested, as expected. The pressures decline slowly and the pressure rise rates decrease faster with increasing particle size. At some size between  $200$  and  $300 \mu\text{m}$ , the narrow sizes of Pittsburgh coal dust can no longer be ignited. These data are typical for narrow size distributions of carbonaceous fuel dusts. A broad size distribution is just a combination of narrow distributions, and these data show that it is the finer particles in a broad distribution that contribute the most to its hazard. The MEC data crosses for the broad size distributions show little difference from the narrow size distribution data below  $D_{\text{med}} \approx 100 \mu\text{m}$ . However, the broad size distributions ignite and propagate at larger  $D_{\text{med}}$  sizes than the narrow size distributions. The pressure and  $dP/dt$  data for the broad size distributions are somewhat higher than those for the narrow size distributions, even in the  $D_{\text{med}}$  range of  $20$ – $100 \mu\text{m}$ . These effects are probably due to the tail of fine particles in the broad size distributions. These fine particles were removed from the narrow size distributions. The main conclusion of Fig. 11 is that particle size has an important effect on the explosibility of coal dusts and other carbonaceous dusts.

Data showing the effect of particle size for iron dust are shown in Fig. 12. Because the size distributions were

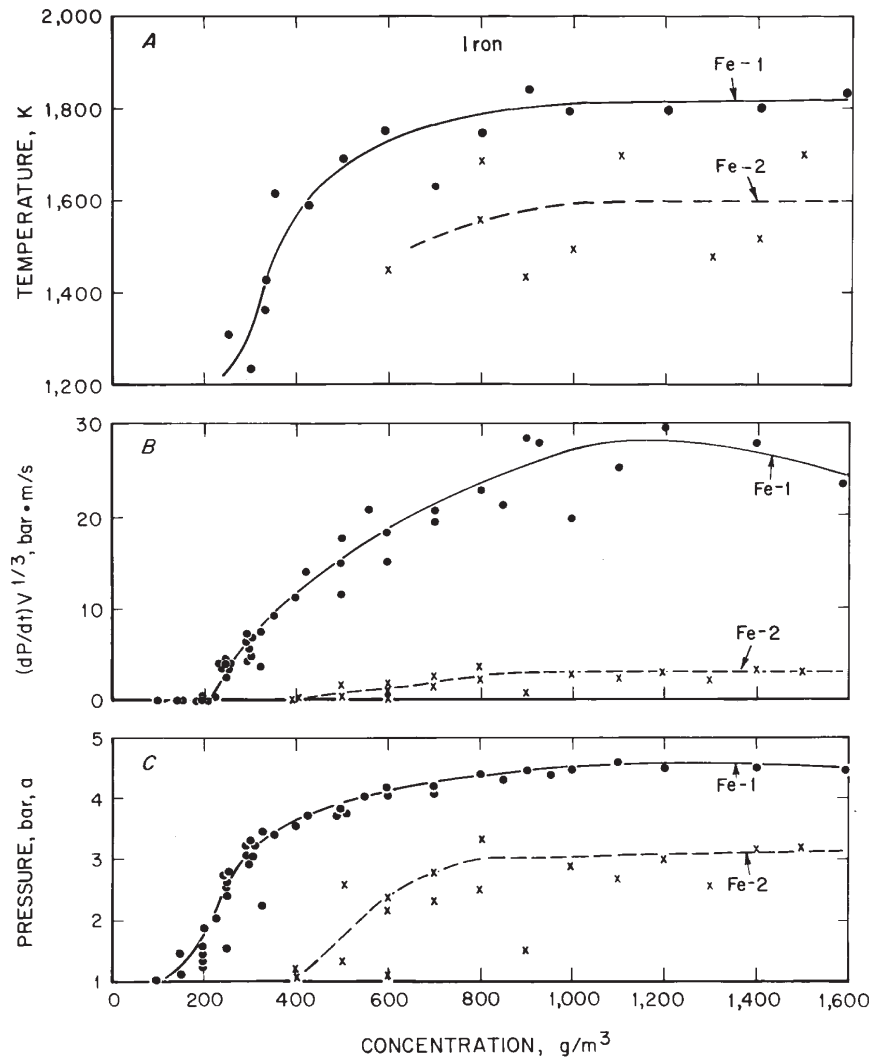


Fig. 10. Explosibility data for two sizes of iron dust.

broader and the  $D_{med}$  values less certain, the data are shown as bars rather than points. The explosion data are similar to those for the coal dust. The maximum values for pressure and rate of pressure rise are found at the finest particle size. The MEC values are relatively size-independent at the finer sizes and increase above  $30\ \mu\text{m}$  until a size is reached that can not be ignited. Additional data for size effects of aluminum dusts are in Cashdollar (1994).

#### 4.4. Effects of oxygen concentration

One of the ways to prevent a dust explosion is to inert the atmosphere so that there is insufficient oxygen for a flame to propagate. This removes one side of the fire triangle or explosion pentagon, thereby preventing combustion. One of the most common inerting gases is nitrogen, which is the main constituent of air. To determine the limiting oxygen concentration for coal dust explosions in the 20-L chamber (with 2500-J ignitors),

the dusts were dispersed with various oxygen–nitrogen mixtures instead of normal air at 20.95%  $\text{O}_2$ . Fig. 13 is an example of the reduced oxygen data for coal dust. The explosions are denoted by the solid circles and the nonexplosions by the open circles. The data for coal dust in air are shown at the top of the figure. In air, the dust ignites and burns at all coal concentrations above the MEC of  $\sim 80\ \text{g/m}^3$ . At the bottom of the figure, explosions still occur at 14% down to 11.5%  $\text{O}_2$ . At 11%  $\text{O}_2$ , the coal dust ignited only in one out of eight tests. At even lower oxygen concentrations, the dust could not be ignited. The boundary between oxygen concentrations that support combustion and those that do not support combustion is the limiting oxygen concentration, LOC. As a safe margin, NFPA 69 (NFPA, 1997) recommends keeping the system oxygen concentration at least 2% lower than the measured LOC. Gases other than nitrogen can also be used to reduce the oxygen concentration. Carbon dioxide is usually more efficient than nitrogen for inerting carbonaceous dusts, but it is often less effec-

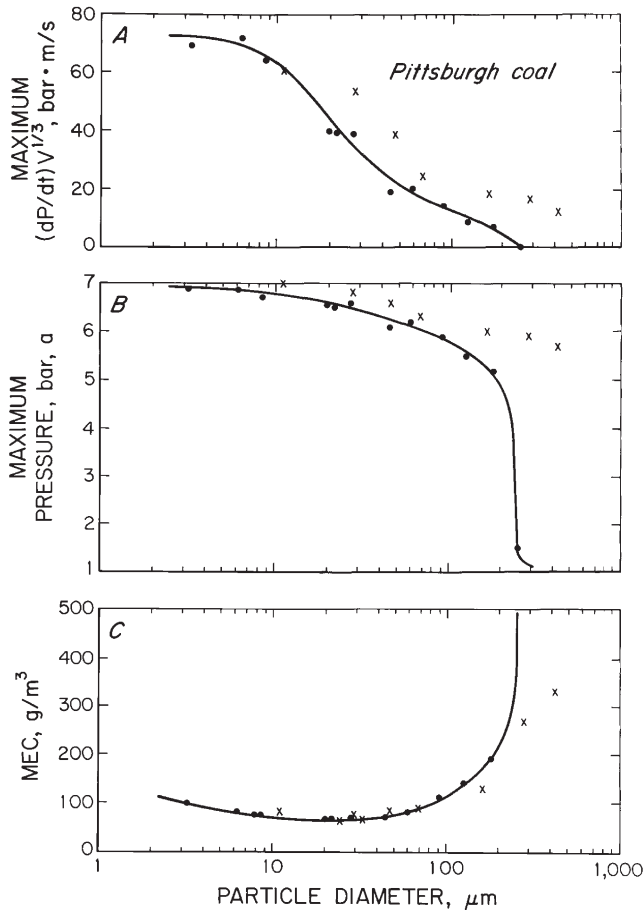


Fig. 11. Effect of particle size on the explosibility of coal dusts: ●, for narrow distributions; ×, for broad distributions.

tive than nitrogen in inerting metal dusts (Nagy, Dorsett & Jacobson, 1964).

The oxidant for a dust explosion is usually the oxygen in air, although other gases can also be oxidizers. Oxygen concentrations greater than 21% tend to increase the burning velocity, and concentrations less than 21% reduce the burning velocity. An example of the effect of varying oxygen concentration on the explosion pressure and rate of pressure rise for a carbonaceous dust is shown in Fig. 14. The data are from DiPalma (1998). The solid data symbols are at a dust concentration of 500 g/m<sup>3</sup> and the open circle data symbols are at a dust concentration of 375 g/m<sup>3</sup>. Fig. 14A shows that the rate of pressure rise varies almost exponentially with oxygen concentration on this semi-logarithmic plot. The explosion pressure in Fig. 14B varies roughly linearly with oxygen concentration, although there is some scatter in the data. If the dust concentration was varied at each oxygen concentration to obtain the highest  $P_{\max}$  value, the explosion pressure would be expected to increase linearly with oxygen concentration, based on the ideal gas law (Eq. (1)). However, this linear relationship would change as the LOC is approached. Near the LOC, the pressure would decrease very rapidly with

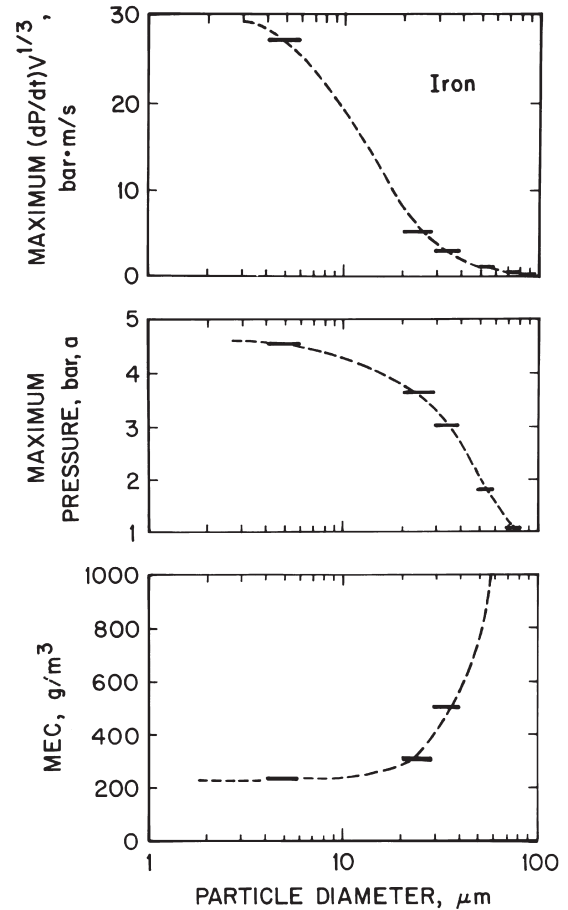


Fig. 12. Effect of particle size on the explosibility of iron dusts.

decreasing oxygen concentration, until the mixture would no longer be explosible.

Because of the large effect of varying oxygen concentration on the explosion characteristics of dusts, it is important to test the dust at the appropriate O<sub>2</sub> concentration. When determining the explosion characteristics for a dust in air, it is important to measure the O<sub>2</sub> content of the “air” cylinders used for the tests. Gas cylinders that are filled with air that has been compressed and dried have the normal 20.95% O<sub>2</sub>. However, many “air” cylinders are filled with synthetic or reconstituted “air” that has been mixed from liquified oxygen and nitrogen. The O<sub>2</sub> content of these cylinders has been observed to vary considerably—from 19% to 26% O<sub>2</sub>.

#### 4.5. Effect of temperature

The thermal ignitability of coal dust is shown in Fig. 15, as measured in the PRL 6.8-L furnace (Conti, Cashdollar & Thomas, 1993). The tests resulting in ignitions (solid circles) and non-ignitions (open circles) are plotted on a graph of initial furnace temperature versus dust cloud concentration. The solid curve is the temperature boundary between the upper region of the graph where

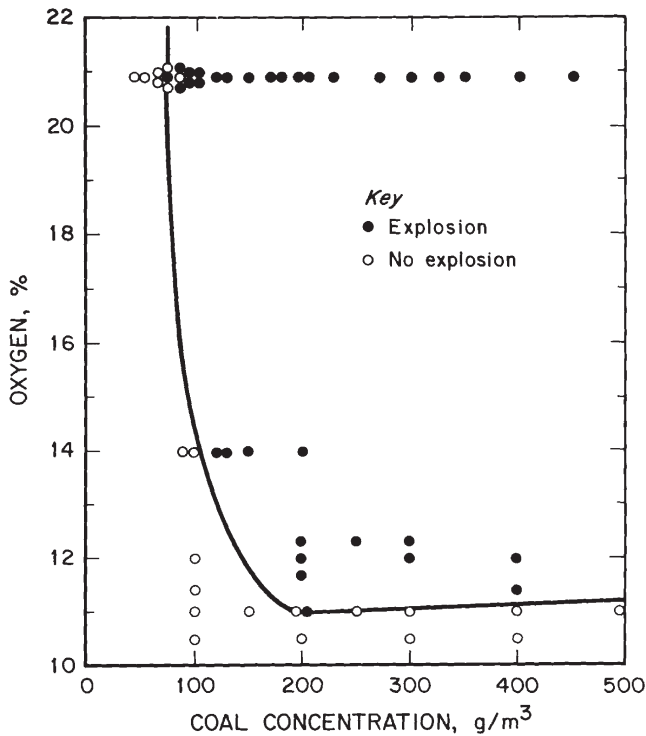


Fig. 13. Effect of reduced oxygen concentration on coal dust explosibility.

the coal dust cloud will thermally autoignite and the lower region where the dust may be flammable but does not thermally autoignite. The lowest point of the curve is the minimum autoignition temperature (MAIT) for the coal—530°C. This 6.8-L furnace is one of several listed in ASTM standard test E1491 for the measurement of the MAIT's of dusts (ASTM, 1999c).

The effect of temperature on the ignitability and explosibility of coal dust is shown in Fig. 16. The dotted curve (from Fig. 15) shows the autoignition temperature for the coal as a function of dust concentration. The dotted curve is the temperature boundary between the upper region of the graph where the coal dust cloud will thermally autoignite and the lower region where the dust may be flammable but does not thermally autoignite. In addition to the 6.8-L furnace data, explosibility tests were also conducted in the 20-L chamber at temperatures above ambient but below the temperature at which the dust would autoignite. For these tests, the 20-L chamber was wrapped with electrical heater tape and insulated to reach the elevated temperature. A thermocouple measured the set temperature of the chamber before the test. The solid circle data points in Fig. 16 show the MEC-data (Cashdollar, 1996) for the coal dust at near ambient (~60°C) and at an elevated temperature of ~180°C. The experimental data points are extrapolated to even higher temperatures (solid curve) using the modified Burgess–Wheeler law (Zabetakis, 1965; Conti, Cashdollar, Hertzberg & Liebman, 1983) for hydrocarbons:

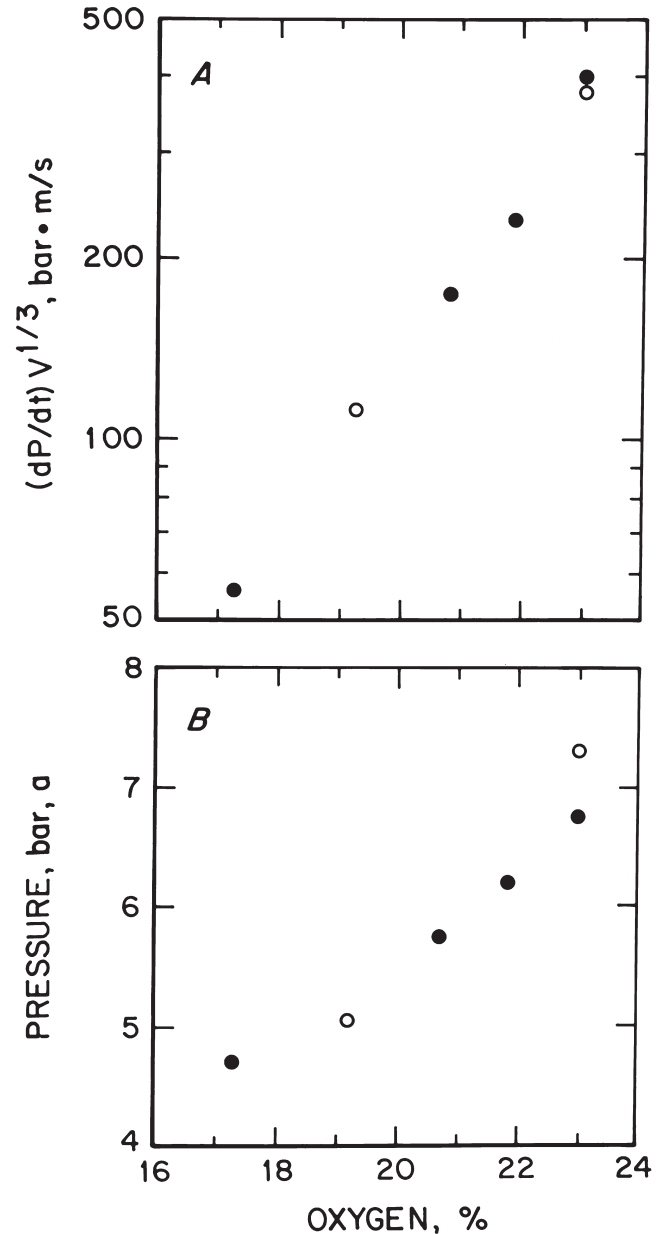


Fig. 14. Effect of oxygen concentration on explosion pressures and rates of pressure rise (data from DiPalma, 1998).

$$C_T = C_{T_0} \left( \frac{273 + T_0}{273 + T} \right) [1 - 0.00072(T - T_0)] \quad (8)$$

where  $C_T$  is the limit in terms of mass concentration at temperature  $T$ ,  $C_{T_0}$  is the limit at  $T_0$ , and the temperatures are in °C. The dust concentrations to the right of the solid curve are flammable (explosible) and the region to the left of the curve is nonflammable. For comparison, the measured lean flammable limit data for methane gas as a function of temperature (dashed curve, from Coward & Jones, 1952, p. 43) are also shown. The decrease in the LFL or MEC with increase in temperature is similar in form for the dust and gas.

At higher dust concentrations, the maximum

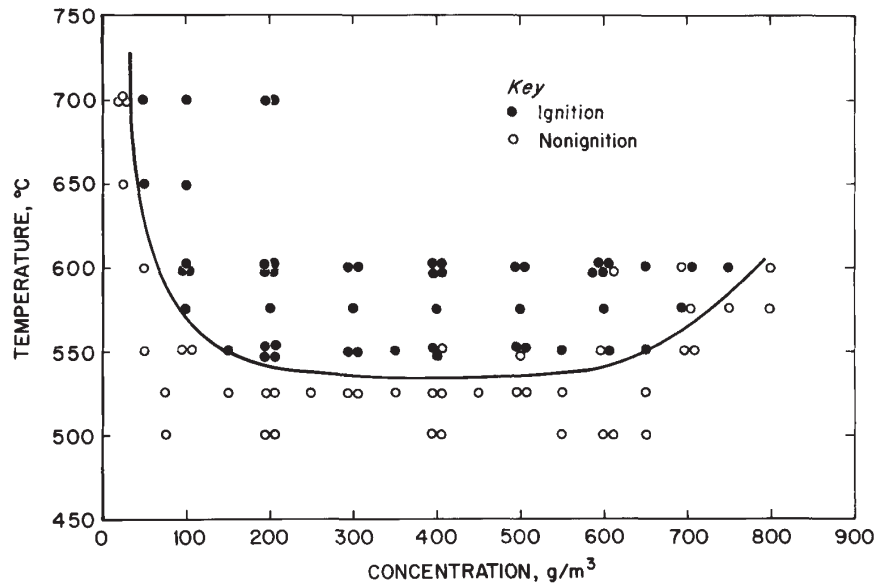


Fig. 15. Thermal ignitability of coal dust.

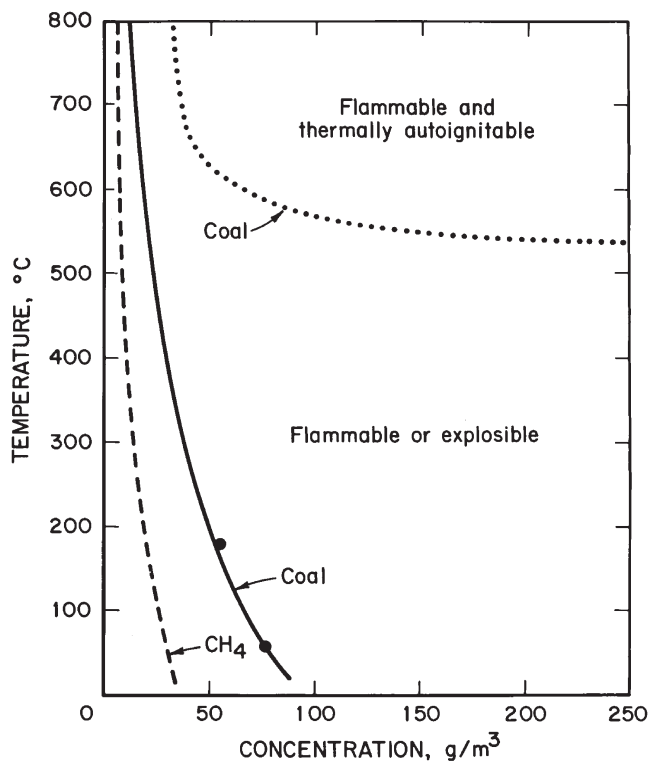


Fig. 16. Effect of temperature on the flammability and thermal ignitability of coal, compared with methane gas.

explosion pressure for the bituminous coal was also measured at elevated temperature in the 20-L chamber (Cashdollar, 1996). At near ambient temperature,  $P_{\max}$  for the dust was 6.6 bar<sub>a</sub>. At an elevated temperature of  $\sim 180^{\circ}\text{C}$ ,  $P_{\max}$  was 4.8 bar<sub>a</sub>. This observation of lower explosion pressures at elevated temperature was also reported previously by Wiemann (1987). The inverse

relationship of explosion pressure with initial temperature is expected from the ideal gas law (Eq. (1)) because there are fewer oxygen molecules at elevated temperature to react with the coal. The ratio of measured maximum explosion pressure (absolute) at elevated temperature to that at ambient temperature is approximately the same as the ratio of ambient to elevated temperature in degrees kelvin.

The limiting oxygen concentration for coal dust was also measured at elevated temperature in the 20-L chamber. The measured LOC value (Cashdollar, 1996) for the dust decreased from  $\sim 11\%$  at ambient temperature to  $\sim 10\%$  at  $\sim 180^{\circ}\text{C}$ . This effect of lower LOC values at elevated temperature was also observed previously by Wiemann (1987).

#### 4.6. Effect of pressure

The effect of initial chamber pressure (Hertzberg et al., 1988a) on the MEC or LFL of gases and dusts is shown in Fig. 17. When the methane concentration is expressed in volume percent in Fig. 17A, the LFL is shown to be constant as the pressure varies from 0.5 to 3 bar. When the  $\text{CH}_4$  is expressed in mass concentration in Fig. 17B, the LFL is shown to vary linearly with pressure. In Fig. 17C, the LFLs of the Pittsburgh coal and polyethylene dusts also vary linearly with pressure. A similar relationship was found by Wiemann (1987) for a brown coal dust.

Bartknecht (1989) and Wiemann (1987) report data on the effect of initial pressure on the  $P_{\max}$  and  $K_{St}$  values. Both show that  $P_{\max}$  increases linearly with increase in initial pressure, over the range of 1–4 bar. They also show that  $K_{St}$  increases with initial pressure.

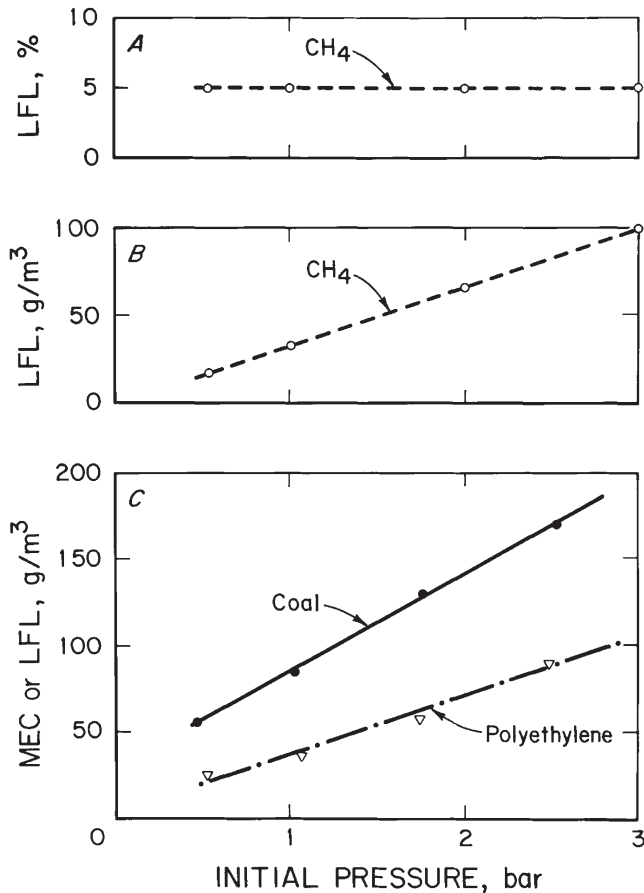


Fig. 17. Effect of pressure on the lower flammable limits for coal and polyethylene dusts, compared with methane gas.

#### 4.7. Hybrid mixtures of dusts and gases

Another important factor in the explosibility hazard of a dust is the possible co-presence of a flammable gas. Hybrid mixtures of a combustible dust (coal) and a flammable gas (CH<sub>4</sub>) were also studied in the 20-L chamber using 2500-J ignitors (Cashdollar, 1996). Data for a low volatile bituminous (lvb) coal are shown in Fig. 18A, and for a high volatile bituminous (hvb) coal in Fig. 18B. The flammable limits for mixtures of coal and CH<sub>4</sub> are shown by the data points and solid curves. The areas above and to the right of the curves are explosible (flammable) and the areas below and to the left of the curves are nonexplosible (nonflammable). The data for mixtures of Pittsburgh coal and CH<sub>4</sub> in Fig. 18B show a linear or near-linear mixing relationship similar to Le Chatelier's Law for hydrocarbon gases (Zabetakis, 1965; Kuchta, 1985, pp. 48–50). All of the solid circle data symbols are for 2500-J ignitors. The measured LFL for the pure CH<sub>4</sub> with this 2500-J ignitor is 4.4%, but this is an overdriven system as shown by tests in a larger 120-L chamber (Hertzberg et al., 1988a). The more appropriate LFL for CH<sub>4</sub> is the 4.9% value measured with a 1000-J ignitor in the 20-L chamber and shown as

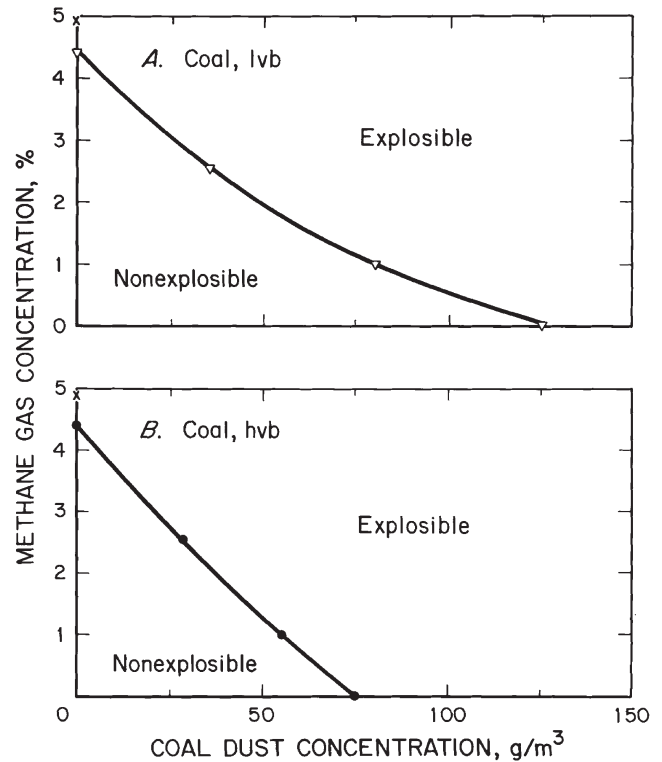


Fig. 18. Lower flammable limits for hybrid mixtures of low and high volatile coal dusts with methane gas.

the symbol  $\times$  in the figure. The data for hybrid mixtures of the low volatile Pocahontas coal and CH<sub>4</sub> in Fig. 18A show some curvature. This is probably due to the even greater difference in ignitability between the low volatile coal and the CH<sub>4</sub>. That is, the dust becomes more easily ignited as more CH<sub>4</sub> is added. Therefore, the curvature is more likely an effect of ignitability rather than an effect of flammability. Ideally, the true mixing relationship would be determined in a much larger chamber, such as a 1-m<sup>3</sup> chamber, where a very strong ignition source could be used for the dusts without overdriving the CH<sub>4</sub> gas. For most practical situations for mixtures of hydrocarbon dusts and gases, the linear mixing law of Le Chatelier would be sufficient. This approximately linear relationship for the lean limits of coal dust and CH<sub>4</sub> gas mixtures was also observed by Amyotte and colleagues (Amyotte, Mintz, Pegg, Sun & Wilkie, 1991; Amyotte, Mintz, Pegg & Sun, 1993) using 5000-J ignitors in a 26-L chamber. This linear mixing relationship is also applicable to mixtures of two carbonaceous dusts (Hertzberg & Cashdollar, 1987). However, it is not applicable to mixtures where the two components have greatly different limit flame temperatures, such as a carbonaceous dust and hydrogen gas (Hertzberg & Cashdollar, 1987).

#### 4.8. Effect of added inert dust

The addition of an inert powder to a combustible dust and air mixture can reduce the explosibility through the absorption of heat. In the mining industry, coal dust explosions are prevented by the addition of limestone rock dust to the deposited coal dust (Nagy, 1981). Since the limestone is incombustible, it acts as a heat sink to reduce the flame temperature of the dust mixture below its limit value. The inerting of coal dust by the addition of limestone rock dust has been studied in the PRL 20-L laboratory chamber, and the results were compared to those from full-scale experimental mine tests (Cashdollar et al., 1992; Cashdollar, 1996; Cashdollar & Hertzberg, 1989; Greninger et al., 1991). The laboratory data are shown in Fig. 19. In the top part of the figure,

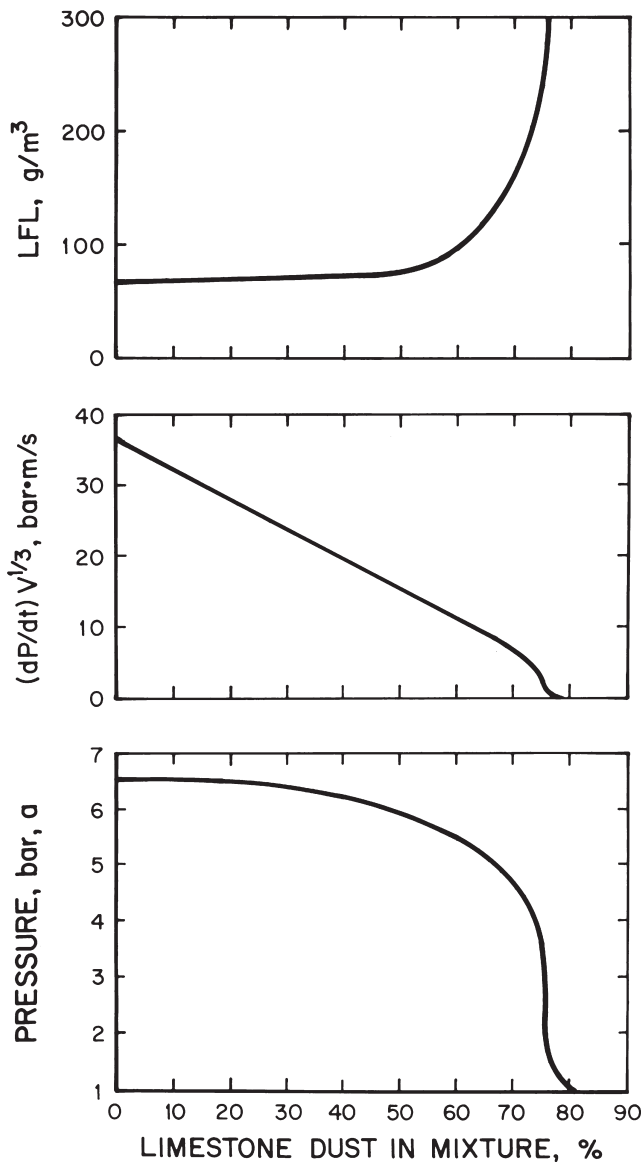


Fig. 19. Effect of added inert dust on the explosion characteristics of bituminous coal dust.

the LFL or MEC of the coal dust shows almost no effect with added rock dust until there is over 50% rock dust in the mixture. At higher rock dust percentages, the LFL increases, until the mixture can not be ignited at  $\geq 75\%$  rock dust. The two lower parts of the figure show the maximum pressure and rate of pressure rise as a function of rock dust percentage in the mixture. At each rock dust percentage, the coal dust concentration was varied over a series of tests to determine the maximum pressure and  $dP/dt$ . The explosion pressures show only a slight decrease with added rock dust content up to about 70%. Between 70% and 80% rock dust, the pressures drop rapidly as the mixture becomes totally inerted and flame no longer can propagate. The rates of pressure rise decline almost linearly with increased rock dust content over the entire range. The 20-L laboratory data for the rock dust inerting of coals shows relatively good agreement with large-scale data from the PRL experimental mine (Cashdollar et al., 1992; Greninger et al., 1991; Weiss et al., 1989). Therefore, the laboratory chamber can be used for preliminary testing to reduce the number of large-scale tests. The mining regulations are still based on the results of the large-scale research.

In addition to the use of inert powders premixed with the combustible dust in order to prevent ignition and flame propagation, inert powders are also used in suppression systems to extinguish propagating explosions.

## 5. Conclusions

The data examples reported in this paper show that laboratory test chambers are useful in studying a wide range of explosion characteristics of dusts. For both carbonaceous and metal dusts, the finer sized dusts are the more hazardous. Because of the importance of particle size, it is critical that representative samples of dusts be collected for explosibility evaluation. Because of the possible accumulation of fines at some location in a processing system, ASTM E1226 (ASTM, 1999a) and E1515 (ASTM, 1999b) recommend that the test sample be less than 200 mesh. It is also important to consider the effects of the initial system temperature, pressure, and oxygen concentration on the explosion characteristics.

## Acknowledgements

The author acknowledges the assistance of G.M. Green in the conduction of the size analyses and the 20-L chamber explosion tests and C.E. Lucci for the computer program for data acquisition and analysis. Both are from the Pittsburgh Research Laboratory of NIOSH. The author also thanks M. Hertzberg (retired from the Bureau of Mines) for introducing him to the subject of dust

explosions and helping him to understand combustion theory.

## References

- Allen, T. (1975). *Particle size measurement*. London: Chapman and Hall.
- Amyotte, P. R., Mintz, K. J., Pegg, M. J., Sun, Y. H., & Wilkie, K. I. (1991). Laboratory investigation of the dust explosibility characteristics of three Nova Scotia coals. *Journal of Loss Prevention in the Process Industries*, 4, 102–109.
- Amyotte, P. R., Mintz, K. J., Pegg, M. J., & Sun, Y. H. (1993). The ignitability of coal dust–air and methane–coal dust–air mixtures. *Fuel*, 72, 671–679.
- ASTM (1999a). Standard test method for pressure and rate of pressure rise for combustible dusts E1226-94. In *ASTM annual book of standards*, vol. 14.02. West Conshohocken, PA: American Society for Testing and Materials.
- ASTM (1999b). Standard test method for minimum explosible concentration of combustible dusts E1515-98. In *ASTM annual book of standards*, vol. 14.02. West Conshohocken, PA: American Society for Testing and Materials.
- ASTM (1999c). Standard test method for minimum autoignition temperature of dust clouds E1491-97. In *ASTM annual book of standards*, vol. 14.02. West Conshohocken, PA: American Society for Testing and Materials.
- Bartknecht, W. (1981). *Explosions: course, prevention, protection*. Berlin: Springer.
- Bartknecht, W. (1989). *Dust explosions: course, prevention, protection*. Berlin: Springer.
- Bartknecht, W. (1993). *Explosions-Schutz (explosion protection)*. Berlin: Springer.
- Cashdollar, K. L. (1994). Flammability of metals and other elemental dusts. *Process Safety Progress*, 13, 139–145.
- Cashdollar, K. L. (1996). Coal dust explosibility. *Journal of Loss Prevention in the Process Industries*, 9, 65–76.
- Cashdollar, K. L., & Chatrathi, K. (1993). Minimum explosible dust concentrations measured in 20-L and 1-m<sup>3</sup> chambers. *Combustion and Science Technology*, 87, 157–171.
- Cashdollar, K. L., & Hertzberg, M. (1982). Infrared pyrometers for measuring dust explosion temperatures. *Optical Engineering*, 21, 82–86.
- Cashdollar, K. L., & Hertzberg, M. (1985). 20-L explosibility test chamber for dusts and gases. *Review of Scientific Instruments*, 56, 592–602.
- Cashdollar, K. L., & Hertzberg, M. (1987). In: Cashdollar, K. L., & Hertzberg, M. (Eds), *Industrial Dust Explosions (Proceedings of the Symposium on Industrial Dust Explosions, Pittsburgh, PA, June 10–13, 1986)*, STP 958 (363 pp). West Conshohocken, PA: American Society for Testing and Materials.
- Cashdollar, K. L., & Hertzberg, M. (1989). Laboratory study of rock dust inerting requirements: effects of coal volatility, particle size, and methane addition. In *Proceedings of the 23rd International Conference of Safety in Mines Research Institutes (September 11–15, 1989, Washington, DC)* (pp. 965–977).
- Cashdollar, K.L., Liebman, I., & Conti, R.S. (1981). Three bureau of mines optical dust probes. US Bureau of Mines RI 8542, 26 pp.
- Cashdollar, K. L., Hertzberg, M., & Zlochower, I. A. (1989). Effect of volatility on dust flammability limits for coals, gilsonite, and polyethylene. In *22nd Symposium (International) on Combustion* (pp. 1757–1765). Pittsburgh, PA: The Combustion Institute.
- Cashdollar, K. L., Weiss, E. S., Greninger, N. B., & Chatrathi, K. (1992). Laboratory and large-scale dust explosion research. *Plant/Operations Progress*, 11, 247–255.
- Conti, R. S., Cashdollar, K. L., & Liebman, I. (1982). Improved optical dust probe for monitoring dust explosions. *Review of Scientific Instruments*, 53, 311–313.
- Conti, R.S., Cashdollar, K.L., Hertzberg, M., & Liebman, I. (1983). Thermal and electrical ignitability of dust clouds. US Bureau of Mines RI 8798, 40 pp.
- Conti, R.S., Cashdollar, K.L., & Thomas, R.A. (1993). Improved 6.8-L furnace for measuring the autoignition temperatures of dust clouds. US Bureau of Mines RI 9467, 26 pp.
- Coward, H.F., & Jones, G.W. (1952). Limits of flammability of gases and vapors. US Bureau of Mines Bulletin 503, 155 pp.
- Deguigand, B., & Galant, S. (1981). Upper flammability limits of coal dust–air mixtures. In *18th Symposium (International) on Combustion* (pp. 705–715). Pittsburgh, PA: The Combustion Institute.
- DiPalma, J. (1998). Cytec Industries, Inc., Stamford, CN, personal communication.
- Dorsett, H.G., Jr., Jacobson, M., Nagy, J., & Williams, R.P. (1960). Laboratory equipment and test procedures for evaluating explosibility of dusts. US Bureau of Mines RI 5624, 21 pp.
- Eckhoff, R. K. (1991). *Dust explosions in the process industries*. Oxford: Butterworth Heinemann.
- Field, P. (1982). *Dust explosions. Handbook of powder technology*, vol. 4. Amsterdam: Elsevier.
- Greninger, N. B., Cashdollar, K. L., Weiss, E. S., & Sapko, M. J. (1991). Suppression of dust explosions involving fuels of intermediate and high volatile content. In *Proceedings of the 4th International Colloquium on Dust Explosions (November 4–9, 1990, Porabka-Kozubnik, Poland)* (pp. 208–228).
- Hertzberg, M., & Cashdollar, K. L. (1987). Introduction to dust explosions. In *Industrial dust explosions, STP 958* (pp. 5–32). West Conshohocken, PA: American Society for Testing and Materials.
- Hertzberg, M., Cashdollar, K. L., & Zlochower, I. A. (1988a). Flammability limit measurements for dusts and gases: ignition energy requirements and pressure dependences. In *21st Symposium (International) on Combustion* (pp. 303–313). Pittsburgh, PA: The Combustion Institute.
- Hertzberg, M., Zlochower, I. A., & Cashdollar, K. L. (1988b). Volatility model for coal dust flame propagation and extinguishment. In *21st Symposium (International) on Combustion* (pp. 325–333). Pittsburgh, PA: The Combustion Institute.
- Hertzberg, M., Zlochower, I. A., & Cashdollar, K. L. (1992). Metal dust combustion. In *24th Symposium (International) on Combustion* (pp. 1827–1835). Pittsburgh, PA: The Combustion Institute.
- Irani, R. R., & Callis, C. F. (1963). *Particle size: measurement, interpretation, and application*. New York: John Wiley and Sons.
- ISO (1985). *Explosion protection systems—Part 1: determination of explosion indices of combustible dusts in air, ISO 6184/1*. Switzerland: International Organization for Standardization.
- Kuchta, J. M. (1985). Investigation of fire and explosion accidents in the chemical, mining, and fuel-related industries—a manual. *US Bureau of Mines Bulletin 680*. pp. 48–50.
- Lewis, B., & von Elbe, G. (1961). *Combustion, flames, and explosions of gases*. New York: Academic Press.
- Mintz, K. J. (1993). Upper explosive limit of dusts: experimental evidence for its existence under certain circumstances. *Combustion and Flame*, 94, 125–130.
- Nagy, J. (1981). The explosion hazard in mining. US Mine Safety and Health Administration IR 1119, 69 pp.
- Nagy, J., & Verakis, H. C. (1983). *Development and control of dust explosions*. New York: Marcel Dekker.
- Nagy, J., Dorsett, H.G., Jr., & Jacobson, M. (1964). Preventing ignition of dust dispersions by inerting. US Bureau of Mines RI 6543, 29 pp.
- NFPA (1997). *Standard on explosion prevention systems, NFPA 69*. Quincy, MA: National Fire Protection Association.
- NFPA (1998). *Guide for venting of deflagrations, NFPA 68*. Quincy, MA: National Fire Protection Association.
- Ng, D.L., Cashdollar, K.L., Hertzberg, M. & Lazzara, C.P. (1983).

- Electron microscopy studies of explosion and fire residues. US Bureau of Mines IC 8936, 63 pp.
- Siwek, R. (1977). 20-L-Laborapparatur für die Bestimmung der Explosionskenngrößen brennbarer Stäube (20-L laboratory apparatus for the determination of the explosion characteristics of flammable dusts). Thesis at Winterthur Engineering College, Winterthur, Switzerland, 109 pp., in German.
- Siwek, R. (1985). *Development of a 20 ltr laboratory apparatus and its application for the investigation of combustible dusts*. Basel, Switzerland: Ciba Geigy AG.
- Siwek, R. (1988). Reliable determination of the safety characteristics in 20-L apparatus. In *Flammable Dust Explosion (November 2–4, 1988, St. Louis, MO)* (pp. 529–573). Holliston, MA: IBC USA.
- Stephan, C.R. (1990). Coal dust as a fuel for fires and explosions. Report No. 01-066-90, US Mine Safety and Health Administration, Pittsburgh, PA, 10 pp.
- VDI (1983). *Pressure release of dust explosions, VDI 3673*. Düsseldorf, Germany: Verein Deutscher Ingenieure.
- Weiss, E. S., Greninger, N. B., & Sapko, M. J. (1989). Recent results of dust explosion studies at the Lake Lynn experimental mine. In *Proceedings of the 23rd International Conference of Safety in Mines Research Institutes, (September 11–15, 1989, Washington, DC)* (pp. 843–856).
- Wiemann, W. (1987). Influence of temperature and pressure on the explosion characteristics of dust/air and dust/air/inert gas mixtures. In *Industrial Dust Explosions, STP 958* (pp. 33–44). West Conshohocken, PA: American Society for Testing and Materials.
- Wolanski, P. (1992). Dust explosion research in Poland. *Powder Technology, 71*, 197–206.
- Zabetakis, M.G. (1965). Flammability characteristics of combustible gases and vapors. US Bureau of Mines Bulletin 627, 121 pp.
- Zhen, G., & Leuckel, W. (1997). Effects of igniters and turbulence on dust explosions. *Journal of Loss Prevention in the Process Industries, 10*, 317–324.